Demography-driven and adaptive introgression in a hybrid zone of the Armeria syngameon

Irene Villa-machío, Myriam Heuertz, Inés Álvarez, Gonzalo Nieto Feliner

Received: 18 July 2022 | Revised: 30 September 2023 | Accepted: 4 October 2023

DOI: 10.1111/mec.17167

ORIGINAL ARTICLE

MOLECULAR ECOLOGY WILEY

Demography-driven and adaptive introgression in a hybrid zone of the *Armeria* syngameon

Irene Villa-Machío[1] | Myriam Heuertz[2] | Inés Álvarez[1] | Gonzalo Nieto Feliner[1]

[1]Department of Biodiversity and Conservation, Real Jardín Botánico (RJB), CSIC, Madrid, Spain

[2]Biogeco, INRAE, University of Bordeaux, Cestas, France

Correspondence
Gonzalo Nieto Feliner, Department of Biodiversity and Conservation, Real Jardín Botánico (RJB), CSIC, Plaza de Murillo 2, 28014 Madrid, Spain.
Email: nieto@rjb.csic.es

Funding information
Spanish Ministry of Science and Innovation-Spanish Agency for Investigation, Grant/Award Number: CGL2017-88500-P; LabEx COTE Fellowship; Investissement d'Avenir, Grant/Award Number: CEBA:ANR-10-LABX-25-01

Handling Editor: Mitchell Cruzan

Abstract

Syngameons represent networks of otherwise distinct species connected by limited gene exchange. Although most studies have focused on how species maintain their cohesiveness despite gene flow, there are additional relevant questions regarding the evolutionary dynamics of syngameons and their drivers, as well as the success of their members and the network as a whole. Using a ddRADseq approach, we analysed the genetic structure, genomic clines and demographic history of a coastal hybrid zone involving two species of the *Armeria* (Plumbaginaceae) syngameon in southern Spain. We inferred that a peripheral population of the sand dune-adapted *A. pungens* diverged from the rest of the conspecific populations and subsequently hybridized with a locally more abundant pinewood congener, *A. macrophylla*. Both species display extensive plastid DNA haplotype sharing. Genomic cline analysis identified bidirectional introgression, but more outlier loci with excess *A. pungens* than *A. macrophylla* ancestry, suggesting the possibility of selection for *A. pungens* alleles. This is consistent with the finding that the *A. pungens* phenotype is selected for in open habitats, and with the strong correlation found between ancestry and phenotype. Taken together, our analyses suggest an intriguing scenario in which bidirectional introgression may, on the one hand, help to avoid reduced levels of genetic diversity due to the small size and isolated location of the *A. pungens* range-edge population, thereby minimizing demographic risks of stochastic extinction. On the other hand, the data also suggest that introgression into *A. macrophylla* may allow individuals to grow in open, highly irradiated, deep sandy, salt-exposed habitats.

KEYWORDS
adaptive introgression, *Armeria*, demography-driven introgression, hybrid zone, range-edge populations, syngameon

1 | INTRODUCTION

The old syngameon concept coined by Lotsy (1925) has been revitalized in recent years (Bog et al., 2017; Cannon & Lerdau, 2015; Cannon & Petit, 2020; Larson et al., 2021). As developed by Grant (1981), the term refers to 'the most inclusive unit of interbreeding in a hybridizing species group', or, in other words, to a group of otherwise distinct species interconnected by limited gene exchange (Suarez-Gonzalez, Lexer, & Cronk, 2018). The term syngameon is related to coenospecies (Turesson, 1922), which Grant (1981) considered an

evolutionarily less inclusive term that he associated with biological species, whereas he associated syngameon with comparium. The syngameon model has been advocated as a likely explanation for how rare tropical tree species with nonspecific pollinators avoid reduced levels of genetic diversity and the Allee effect, which is a demographic challenge (Cannon & Lerdau, 2015, 2019). Evolutionary advantages of the syngameon have also been proposed for the most diverse northern temperate tree genus, *Quercus*, in which episodic exchange of genetic material is interpreted as a strategy for adaptation to changing environmental conditions (Cannon & Petit, 2020). Advantages for island colonization have also been attributed to these networks of interfertile species (Caujapé-Castells et al., 2017).

The structure of syngameons is not homogeneous. Using simulation studies, Boecklen (2017) found nonrandom variation in the propensity to hybridize, meaning that some species hybridize more frequently than others, which is consistent with the classical compilospecies concept, in which one species captures parts of the genome of several other sympatric species through introgression (Fuertes et al., 1999a; Harlan & De Wet, 1963; Stebbins, 1971).

The question of how species maintain their cohesiveness despite frequent or occasional gene flow has focused most of the attention regarding syngameons (Kremer & Hipp, 2020). In the *Symphonia* tropical tree syngameon for example, empirical data suggest an interplay of within-species adaptive processes and between-species differential adaptation, with relaxed competition at species niche margins, to explain coexistence of its species and the overall evolutionary success of the syngameon (Schmitt et al., 2020, 2021). However, persistent hybrid lineages with evolutionary potential may also form within these networks, as in the Lousiana *Iris* syngameon (Arnold et al., 2004). Accordingly, syngameons can also be considered as networks of interbreeding species that can provide different benefits to their members and thus lead to different evolutionary outcomes. This raises the question of what factors favour the evolutionary fate of hybrid populations within syngameons.

Assessing evolutionary scenarios within syngameons requires accurate inference of introgression, the transfer of genes between species mediated primarily by backcrossing (Anderson, 1949; Heiser, 1973). Past introgression has traditionally been inferred from incongruence between nuclear and organellar phylogenies (Rieseberg & Wendel, 1993; Wendel et al., 1995) and, more reliably, using phylogenomic approaches (Hibbins & Hahn, 2022). As a result, introgression is essentially known from its genetic consequences rather than from the ongoing process itself and its driving factors (Hamlin et al., 2020; Pfennig, 2021). Understanding the genetic, demographic, and ecological factors that influence the early and intermediate stages of introgression, where backcrossing leads to allele transfer (Abbott et al., 2016; Suarez-Gonzalez, Hefer, et al., 2018), could shed light on evolutionary scenarios within syngameons and on their long-term consequences. Thus, focusing on groups where both past and current hybridization occur, and where different outcomes of hybridization have been recorded, can potentially help fill the knowledge gap between patterns and drivers of hybridization and introgression through time.

Armeria (Plumbaginaceae) is a primarily Mediterranean genus consisting of c. 100 strictly outcrossing species (Baker, 1966) with generalist pollinators (García-Camacho et al., 2009; Herrera, 1987) and can be considered a syngameon. There is abundant evidence of current and past hybridization within this genus. Numerous cases of recent or ongoing introgression have been reported (Baumel et al., 2020; Fuertes et al., 1999b; Lefèbvre, 1969, 1974; Nieto Feliner et al., 2019; Philipp et al., 1992; Piñeiro et al., 2011; Tauleigne-Gomes & Lefèbvre, 2005, 2008). In addition, there is evidence that hybridization was involved in the origin of taxa such as *A. carratracensis* (Nieto Feliner et al., 1996, 2002), *A. salmantica* (Nieto Feliner, 1997), *A. trianoi* (Nieto Feliner et al., 2001), and there is ecomorphogeographical evidence for many others (Nieto Feliner, 1990). At the multispecies level, sharing of molecular variants across species due to hybridization, i.e., species-independent geographically structured patterns of variation, has been found at both large and fine spatial scales for nrDNA ITS (Fuertes et al., 1999a; Fuertes & Nieto Feliner, 2003; Nieto Feliner et al., 2004) and plastid DNA sequences (Gutiérrez Larena et al., 2002). Applying the term syngameon to the entire genus may seem excessive since not all *Armeria* species throughout the genus range are currently connected by gene flow in a single network of interfertile species. However, almost all attempts to create synthetic hybrids, including our own involving 20 taxa, have produced fertile F1 progeny (Nieto Feliner, 1997; Nieto Feliner et al., 1996), and the Iberian Peninsula, where two thirds of the species are concentrated (Nieto Feliner, 1990), has probably been a suitable arena for hybridization resulting from episodic or recurrent contacts between species ranges.

This study focuses on a hybrid zone between *Armeria pungens* and *A. macrophylla*. *Armeria pungens* is a coastal sand dune species restricted to the southwestern Iberian Peninsula and to two smaller disjunct areas, an offshore island in NW Spain and Corsica–Sardinia (Piñeiro et al., 2007). The species exhibits evidence of past or ongoing introgression from subcoastal *Armeria* species at the northern and southern edges of its core distribution range (Piñeiro et al., 2011). In our study area in the southernmost part of its range, introgression toward *A. pungens* from a pinewood and shrubland congener, *A. macrophylla*, was revealed based on nrDNA ITS and plastid DNA (*trn*L-*trn*F) sequences, and this interpretation is consistent with genome size, 45S and 5S rDNA locus-FISH data, nrDNA IGS sequences, AFLP and morphometric data (Nieto Feliner et al., 2019; Piñeiro et al., 2007, 2011). *Armeria macrophylla* occurs along a subcoastal fringe in the southwest of the Iberian Peninsula (Nieto Feliner, 1990). The hybrid zone is located in Punta Camarinal, a coastal site bordering the Gibraltar Strait. It exhibits a single plastid haplotype, based on sequences from three noncoding regions that are shared by both species and not found elsewhere (Nieto Feliner et al., 2019), strongly suggesting a plastid capture event (Acosta & Premoli, 2010; Rieseberg, 1995). Genetic and morphometric variation and the spatial distribution of the two species in the area point to a hybrid zone in which habitat seems to be a better predictor of the morphological phenotype of each individual than ITS sequences. Overall, this hybrid zone appears to be a very interesting system in

which the genomic and geographic structure of hybridization and introgression and their driving factors are insufficiently understood.

The overarching questions of this study are (1) whether and how different evolutionary outcomes occur within syngameons and (2) whether the study of a hybrid zone within a syngameon can provide insights for interpreting its complex reticulate phylogenetic patterns. To address these questions, we focus on the hybrid zone between *A. pungens* and *A. macrophylla* and formulate the following specific objectives. What are the levels, direction(s), and drivers of introgression? Are there signatures of selection, suggesting adaptation to environmental factors? What is the demographic history of the populations of the two species? Can we confirm a plastid capture at the study site, as suggested by Sanger sequencing evidence? We investigated these questions using ddRAD data and reconstructed the evolutionary history of this hybrid zone.

2 | MATERIALS AND METHODS

2.1 | Study system

The study site, Punta Camarinal, is a small coastal headland in the Gibraltar Strait area near Tarifa, Atlantic Ocean (Cádiz, Spain), flanked by two beaches, El Cañuelo to the west and Bolonia to the east, the latter forming a 30 m high dune that enters into the headland (Figure 1a). Most of the site is covered by a *Pinus pinea* pinewood planted in the late 1950s to stabilize this dune, but the area was previously dominated by macchia shrubland, with patches of pinewoods. Macchia shrubland currently borders the pinewood along the coast, especially to the west, and is separated from the beach by a narrow strip of highly exposed open vegetation that extends inland in the southern part. This open vegetation grows on loose sand or fossil dunes, but all three habitats —pinewood, shrubland and open vegetation— occur on sandy soils. Sampling undertaken in 2017 and 2018 included 115 individuals from Punta Camarinal covering the three habitats as well as 20 individuals from each of the two nearest populations of the hybridizing species (Cape Trafalgar for *A. pungens* and Barbate for *A. macrophylla*; Table S1; Figure S1). In addition, three individuals of *A. hirta* from a close (c. 2 km away) population were sampled as an outgroup. In total, we collected fresh leaves in silica gel and flowering fragments from specimens for morphometric analysis from 158 individuals, all of which were georeferenced and photographed.

2.2 | Morphometric analysis

To assess phenotypic variation across the study site and in the closest populations of the two hybridizing species, we performed a morphometric analysis on the same individuals ($n = 155$) sampled for the genomic study. Sixteen quantitative variables were used, following Piñeiro et al. (2011) (Table S2). Three of them are ratios. To maximize independence of variables, we kept only one of the two variables used in each ratio for the analyses. Principal component analysis (PCA) was performed to reduce the dimensionality of the data and to explore morphometric variation relative to genomic patterns, especially hybrid classes.

Nonparametric Spearman's rho correlation tests were performed on the Camarinal samples to examine the association between habitat, categorically defined as open versus pinewood or shrubland, and phenotype, represented by the scores for PC1 from the morphometric PCA (*A. pungens* phenotype with PC1 < 0, *A. macrophylla* phenotype with PC1 > 0). The correlation between habitat and ancestry, as estimated from STRUCTURE (see below), was also estimated to assess whether plasticity played a role. To control for potential bias due to the higher number of *A. macrophylla* samples, these two tests were performed on a subsampled dataset containing equal numbers of genetically pure *A. macrophylla* and *A. pungens*, but all admixed samples. Analyses were performed using IBM SPSS Statistics for Windows version 28.0 (IBM, Armonk, NY, USA).

2.3 | DNA sequencing and bioinformatics analysis

Genomic data were generated for all 158 individuals of *A. pungens*, *A. macrophylla*, hybrid individuals and *A. hirta*. Total DNA was extracted from dried leaves following the CTAB protocol (Doyle & Doyle, 1987) and processed to obtain genomic libraries using a low-cost double-digest restriction site-associated DNA sequencing approach (low-cost ddRADseq) based on Kess et al. (2016). Paired-end libraries were quantified using the Qubit dsDNA HS Assay (Thermo Fisher Scientific) and sequenced on an Illumina HiSeq X PE150 platform. Demultiplexed reads were inspected using FastQC 0.11.5 (Andrews, 2010) for quality control, and filtered with Trimmomatic 0.36 (Bolger et al., 2014) to remove adapters (ILLUMINACLIP:TruSeq3-PE-2.fa:2:30:10).

High-quality ddRADseq reads from 155 samples of *A. pungens*, *A. macrophylla* and hybrid individuals were de novo assembled using ipyRAD v. 0.7 (Eaton & Overcast, 2020) on the high-performance computing cluster Trueno (SGAI-CSIC, Madrid, Spain). The similarity threshold for individual sequence assemblies was set at 88%, both within and between samples, considering only loci with a maximum of two alleles per sample, with a minimum sequence depth of 8. Loci present in at least 90% of the samples were retained, and the remainder were discarded. Because different genetic regions may be exchanged at different rates between hybridizing species, individuals from a hybrid zone could accumulate higher heterozygosity than expected under random mating. Accordingly, to account for a hybrid zone scenario, several assemblies were built with different thresholds for heterozygous genotypes per site and per ddRADseq locus across the dataset (0%, 20%, 40%, 60%, 80%). For example, if a given site at a given locus was heterozygous in 25% of the samples, that locus would be eliminated in the assembly with the 20% heterozygosity threshold but retained in the assembly with the 40% threshold. To select the most appropriate assembly, we plotted the number of loci retained in each assembly and selected the one in which the

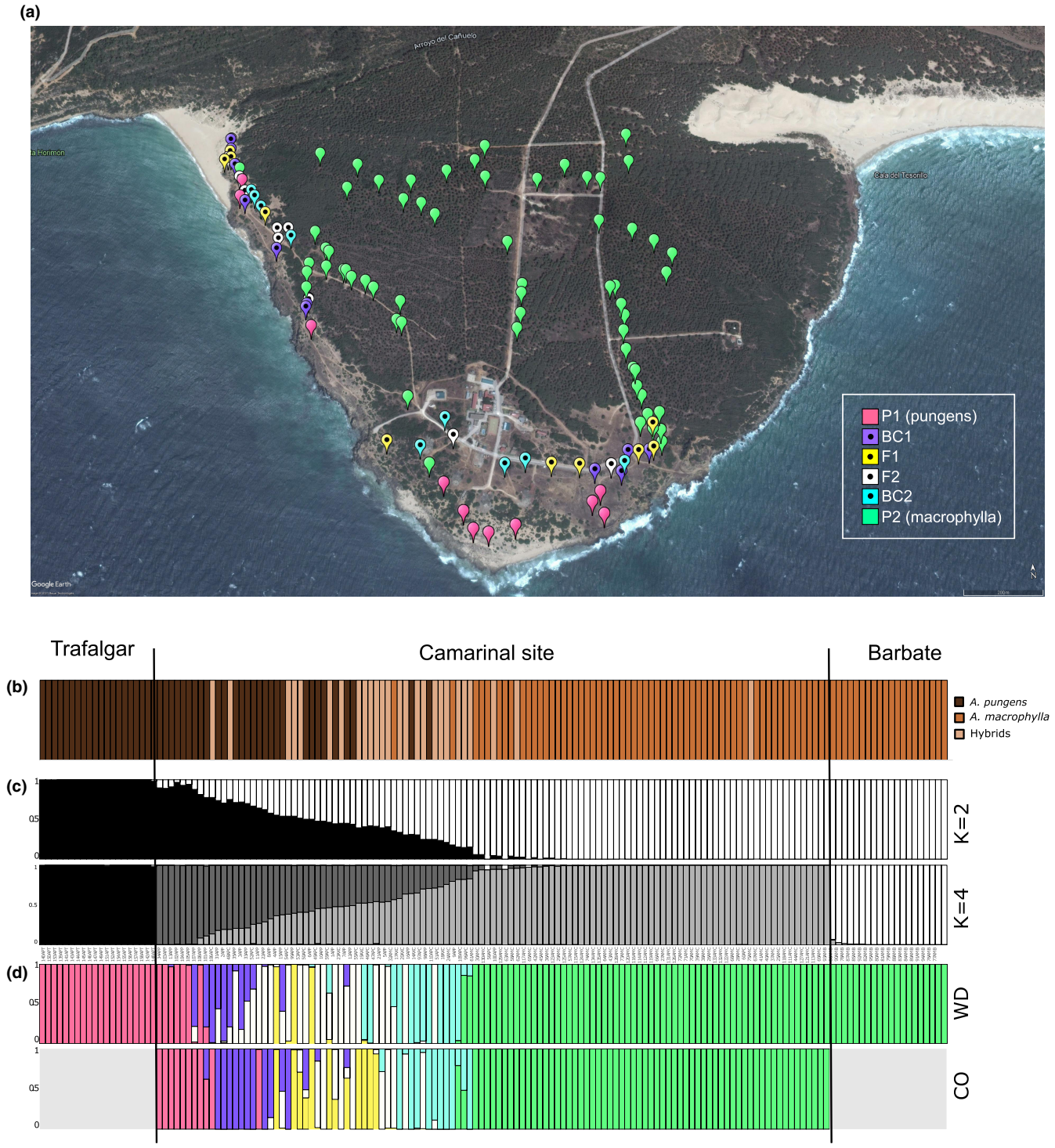

FIGURE 1 (a) Sampling of 115 specimens of *Armeria* in a hybrid zone between *A. pungens* and *A. macrophylla* in Punta Camarinal (Cádiz, Southern Spain), labelled by genotypic classes according to NewHybrids analysis of the Camarinal only (CO) dataset. Colour code represents the genotypic class to which the individual had the highest posterior probability of being assigned. (b) Field taxonomic identification of the 155 samples (*A. pungens*, *A. macrophylla*, hybrid). (c) Bayesian genetic clustering using STRUCTURE of 155 samples including two geographically close populations (*A. pungens* from Cape Trafalgar; *A. macrophylla* from Barbate); optimal ($K=2$) and suboptimal ($K=4$) partitions. (d) Assessment of genotypic classes using NewHybrids of 155 samples (whole dataset, WD) and 115 samples (CO).

number of loci plateaued (Scott et al., 2019), which turned out to be the assembly with the 60% heterozygosity threshold (Figure S2). With these parameters, we generated an assembly and genotyping matrix of 4412 biallelic SNPs from the 155 samples, referred to as the whole dataset (WD), i.e., including the two external populations of *A. pungens* and *A. macrophylla*, and all the samples from the study site (Camarinal). The Camarinal only (CO) subset of the genotyping matrix was restricted to the 115 samples from Camarinal (Table S1).

2.4 | Population genetic structure and diversity

To visualize the distribution of genetic diversity of *A. pungens* and *A. macrophylla*, a PCA was performed on the WD dataset using the 'adegenet' package (Jombart & Ahmed, 2011) in the R environment (R Core Team, 2015). Evolutionary relationships between individuals were also assessed, taking into account uncertainty due to hybridization, using a Neighbour-Net analysis based on uncorrected p-distances performed in SplitsTree V4.16.1 (Huson & Bryant, 2006). Population genetic structure was inferred using a Bayesian model-based genetic clustering approach in STRUCTURE v2.3.4 (Pritchard et al., 2000) under an admixture model with correlated allele frequencies, based on one SNP per locus, for a total of 614 SNPs. Each number of genetic clusters K (1–6) was assessed five times, running 10^6 iterations, in addition to 10^5 as burn-in, and the results combined in the online application CLUMPAK (http://clump ak.tau.ac.il/). The optimal partition was estimated using the Evanno criterion (Evanno et al., 2005) implemented in Structure Harvester (Earl, 2012). To obtain a finer estimate of hybrid classes, we used NewHybrids v1.1 (Anderson & Thompson, 2002), which computes the posterior probability distribution that each sample falls into one of six genotypic classes: parental classes P1 and P2, first and second-generation hybrids F1 and F2, and backcrosses to both parental classes, BC1 and BC2. Due to computational limitations of NewHybrids, we used the gl.nhybrids function in the dartR package (Gruber et al., 2018) to downsample the two datasets by selecting a reduced number of suitable unlinked loci, resulting in 151 SNPs being retained for the two datasets. We did not use any prior information on sample assignment to parental classes (P1, P2) in NewHybrids and performed an analysis with default parameters and 50,000 MCMC steps after 10,000 burn-in steps on each of the two datasets (WD and CO). For some downstream analyses, five groups of individuals were defined based on the NewHybrids analysis of WD: pure *A. pungens* from Trafalgar, pure *A. pungens* from Camarinal, pure *A. macrophylla* from Barbate, pure *A. macrophylla* from Camarinal, and a single group of hybrids consisting of all individuals of the hybrid classes F1, F2, BC1, and BC2 from Camarinal. Nucleotide diversity within and pairwise differentiation between these groups (F_{ST}) were estimated using the Popgenome package (Pfeifer et al., 2014) in the R environment. In addition, expected heterozygosity per group (H_e) was estimated using vcftools (Danecek et al., 2011).

2.5 | Genomic introgression

To investigate differential patterns of introgression across the genome in the hybrid zone, we used the Bayesian genomic cline model implemented in bgc (Gompert & Buerkle, 2011), which quantifies locus-specific patterns of introgression and identifies outlier loci that show an excess of introgression relative to the genomic average. The α parameter indicates the direction of introgression. For each locus, it denotes an increase (for positive values) or decrease (for negative values) in the probability of *A. macrophylla* ancestry relative to the expectation, i.e., the individual's hybrid index. The β parameter estimates the rate of change per locus, i.e., it describes an increase (steeper cline) or decrease (wider cline) in the rate of transition from *A. pungens* to *A. macrophylla* ancestry along the hybrid index or genome-wide admixture gradient. Genomic cline analyses were performed on the two datasets, filtering to discard loci with minor allele frequency <0.05 and retaining only one SNP per assembled RADseq locus, resulting in 553 SNPs. For WD, we fitted the bgc model for 115 individuals from the Camarinal hybrid zone, using *A. pungens* from Trafalgar ($N=20$ samples) and *A. macrophylla* from Barbate ($N=20$ samples) as parental reference populations. For the CO dataset, we fitted the bgc model for 45 admixed individuals from Punta Camarinal, using as parental references non-admixed samples according to the analysis of the WD dataset, i.e., *A. pungens* (P1, $n=7$), *A. macrophylla* (P2, $n=63$), which is more stringent in identifying a sample as pure. A genotype uncertainty model was used as recommended for next-generation sequence data (Gompert & Buerkle, 2011), with the sequencing error rate estimated previously by the ipyRAD software (0.003). The models were fitted with five chains of MCMC, each with 25,000 iterations, a 5000-iteration burn-in, and a thinning interval of 5. The five chains were combined after checking the convergence of the MCMC chains. Loci were considered outliers if they met the two criteria described by Gompert and Buerkle (2011), namely that the 95% credible intervals for α or β did not overlap zero and that the median of the posterior distribution was not contained in the interval bounded by the 1–0.95/2, 0.95/2 quantiles of the probability distribution. The bgc output was visualized using the ClineHelpR package (Martin et al., 2021) in the R environment. Outlier loci were annotated using blastn on the NCBI website (https://blast.ncbi.nlm.nih.gov/Blast.cgi).

We tested for the possibility of non-recent introgression that may have gone undetected with the four-taxon *D*-statistic metric (Durand et al., 2011), as integrated in the ABBA-BABA ipyrad analysis toolbox v.0.9.81 (Eaton, 2014; Eaton & Ree, 2013), using only those samples identified as nonhybrid by the NewHybrids analysis of WD. In a four-taxon pectinate tree [(((P1, P2), P3), P4)], where A and B represent ancestral and derived alleles, respectively, the P3 taxon is expected to share derived alleles with either sister species, P1 (BABA) or P2 (ABBA) in the same proportion. An excess of BABA or ABBA patterns is interpreted as evidence of ancient admixture between lineages. Two scenarios were tested (Figure S3) after inferring a maximum likelihood tree using the ipa.raxml module of ipyrad and rapid bootstrap support estimated from 10 replicate searches using the GTRGAMMA nucleotide substitution mode: the first with P1 = *A. pungens* (Trafalgar), P2 = *A. pungens* (Camarinal), P3 = *A. macrophylla* (Camarinal), P4 = *A. hirta*, and the second with P1 = *A. macrophylla* (Barbate), P2 = *A. macrophylla* (Camarinal), P3 = *A. pungens* (Camarinal), P4 = *A. hirta*. For the introgression test, we generated 60 replicates for each of the two scenarios, where each replicate (test) combined different samples from P2 and P3 representing the same terminal taxon with the same set of P1 samples. Significance was assessed through 1000 bootstrap replicates for each test, and the *Z*-score was calculated

to measure the number of bootstrap standard deviations where the *D*-statistic deviates from zero. Tests were considered significant for a *Z*-score >2.58, corresponding to a conservative cutoff of $\alpha = 0.01$ after correcting for multiple comparisons using the Holm–Bonferroni correction (Eaton & Ree, 2013).

2.6 | Demographic analyses

To investigate the origin of the hybrid zone, we used coalescent modelling to infer the demographic history of the hybridizing species, focusing on non-hybrid individuals at the study site and external populations. We used two complementary approaches based on the site frequency spectrum (SFS) to infer the demographic history of *A. pungens* and *A. macrophylla* in the region, focusing on the 108 non-hybrid individuals resulting from the NewHybrids analysis of WD. Samples were divided into four groups: 20 *A. pungens* from Trafalgar, 20 *A. macrophylla* from Barbate, and 7 *A. pungens* and 61 *A. macrophylla* from Camarinal. The resulting dataset was pruned of variants that could be in linkage using plink v1.90p (Purcell et al., 2007) with the following arguments: a window size of 50 kb, a window step size of 10 bp, and a linkage threshold r^2 of 0.1; that is, for any pair of variants with r^2 greater than 0.1, only one variant was retained. After this pruning, the dataset contained 1271 SNPs. To construct the folded SFS, we used easySFS (https://github.com/isaacovercast/easySFS) and downsampled our dataset to a smaller number of samples per group (7 samples, i.e., 14 alleles) to allow for balanced sample sizes across groups.

The first approach was to estimate changes in population size over time in each of the four genetic groups, particularly recent events of population expansion or decline. To do this, we generated Stairway plots (Liu & Fu, 2015). Singletons were ignored, and the default parameter values were used (200 SFS input files and 67% of sites used for training). We used a mutation rate of 5.265×10^{-9}, the average evolutionary rate of eight angiosperm families calculated by De La Torre et al. (2017), and a generation time of 5 years.

The second approach aimed to reconstruct the population demographic history of the two hybridizing species in the study region, and to analyse and describe their changes over time through hypothesis-driven demographic simulations. For this purpose, we used Fastsimcoal2 version 2.6.0.3 (Excoffier et al., 2013). Five demographic models exploring interspecific gene flow were simulated (Figure S4), considering: (1) continuous gene flow since the onset of divergence between *A. pungens* and *A. macrophylla* (only two genetic pools, i.e., populations of each of the two species merged); (2) four groups with no gene flow; (3) recent gene flow between *A. pungens* and *A. macrophylla* at the Camarinal site since population divergence in *A. macrophylla* (Barbate vs. Camarinal); (4) early gene flow between *A. pungens* and *A. macrophylla* at the Camarinal site since population divergence in *A. pungens* (Trafalgar vs. Camarinal site); (5) same scenario as 4 but including a bottleneck event in the Camarinal population of *A. pungens*, specifically, an instantaneous population size reduction starting at TBOT and lasting 500 generations into the past. The last model was added, despite the fact that such a bottleneck remained undetected in Stairway plots (see Results), because models 3 and 4 consistently yielded N_e estimates for *A. pungens* that were an order of magnitude smaller in Camarinal than in Trafalgar. Several parameters were estimated such as population size, divergence times, and migration rates between populations in Punta Camarinal. Each model was run 40 times, using 500,000 coalescent simulations to calculate the composite likelihood and 60 cycles of expectation–conditional maximization (ECM). Runs with the highest likelihood in each model were retained and the Akaike Information Criterion (AIC) was calculated to determine the probability of each model. These values were compared to determine the most likely demographic model (Excoffier et al., 2013). Point estimates of the demographic parameters for the selected model were extracted from the run with the highest likelihood. To estimate the confidence intervals for these parameters, 150 SFS from the run with the highest composite likelihood were simulated, with 20 runs per simulated SFS. Runs with the highest maximum likelihood for each simulated SFS were used to define the 95% CI values.

2.7 | Plastid genome analysis

To investigate the occurrence of plastid capture at the study site, we first sequenced the plastome of a sample of *A. pungens* from the Trafalgar population. Library construction and assembly were performed at AllGenetics & Biology SL (A Coruña, Spain). A total DNA library was constructed using the Nextera XT DNA Sample Prep kit (Illumina) according to the manufacturer's instructions. The library was sequenced on a fraction of a lane on an Illumina MiSeq instrument, yielding paired-end 300 bp reads. The raw fastq files were quality checked in FastQC 0.11.3, and duplicated reads were removed using the clumplify.sh script from the BBmap package 37.00. Trimmomatic 0.36 (Bolger et al., 2014) was used to remove adapters and low quality regions. A de novo assembly was generated by using SPAdes 3.11 (Bankevich et al., 2012), which was compared against the NCBI nt nucleotide database using blastn, a BLAST+ 2.6.0 program (Camacho et al., 2009), with the following parameters: e-value 1e-4, max target seqs 50, max hsps 1. Scaffolds with at least 80% of hits to plastid DNA were listed and extracted from the assembly. QUAST 4.4 (Gurevich et al., 2013) was used to check the assembly quality of the plastid scaffolds. Then, complete plastid genome references which had high blastn similarity to the *A. pungens* plastome scaffolds were identified from NCBI.

Plastid DNA polymorphism was analysed in $n = 158$ samples, including the three samples of *A. hirta*. ddRADseq data were mapped against the plastid reference genome of *A. pungens*, using the *mem* algorithm of BWA (Li & Durbin, 2009) with default settings. Mapped reads were filtered using SAMtools (Li et al., 2009) *view* and *sort* with default parameters. SNPs were called using SAMtools *mpileup* and VarScan2 *mpileup2snp* (Koboldt et al., 2012) with minimum variant

allele frequency threshold of 0.5, minimum base quality of 30, minimum read frequency of 0.5 to call homozygotes and minimum read depth of 3. Plastid SNPs were filtered and cleaned using VCFtools (Danecek et al., 2011) to retain only SNPs with a minimum read depth of 5, a minimum genotype quality of 10, a maximum of 30% missing data, and only biallelic sites. All indels were removed. Missing data were imputed using Beagle (https://faculty.washington.edu/browning/beagle/beagle.html; Browning & Browning, 2007). The number of haplotypes, and a median-joining haplotype network showing the relationships between them, were analysed using PopART (Leigh & Bryant, 2015).

3 | RESULTS

3.1 | Morphometric analysis

The PCA of the morphometric variables in the whole dataset resulted in five PCs with eigenvalues greater than one. The first two explained 51.95% of the variance (28.09% and 23.86%, respectively). Variables contributing more to the first PC included both vegetative and reproductive traits related to the scape (stems), involucral bracts, and calyces (Table S2). In the scatterplot against the first two PCs, the samples were distributed on either side of the bidimensional space with some discontinuity (Figure S5). Negative values for PC1 corresponded to an *A. pungens* phenotype, whereas positive values corresponded to an *A. macrophylla* phenotype. Labeling of samples based on the NewHybrids classification of WD showed that the *A. pungens* morphospace included all six genotypic classes, even non-admixed *A. macrophylla* (P2) samples. In contrast, the *A. macrophylla* morphospace included mostly P2 samples, in addition to five backcrosses (BC2) and four F2s. In the Camarinal site, phenotype was significantly correlated with habitat ($rs = -0.458$, $p < .01$), such that plants growing in open habitats mostly exhibited an *A. pungens* phenotype whereas those occurring in pine or shrubland understory mostly exhibited an *A. macrophylla* phenotype (Figure S6). Ancestry was also strongly correlated with habitat ($rs = 0.477$, $p < .01$).

3.2 | Assembly and bioinformatic filtering of genomic data

In total 173,861,569 raw reads were obtained from 155 samples of the whole dataset WD, with an average of 1,121,687.54 raw reads per sample (253,428–2,369,788 reads). WD included 614 loci (tags) with 4412 biallelic SNPs.

3.3 | Population genetic structure

In the PCA based on 4412 biallelic SNPs, the first two PCs accounted for 51.23% of the total variance (43.5% and 7.73, respectively, Figure 2). The scatterplot of the samples against the first two PCs, labelled according to the NewHybrids results of WD, showed that non-admixed *A. pungens* from Camarinal ($n = 7$ samples) were genetically distinct from those of the Trafalgar population. This was in contrast to *A. macrophylla*, where samples from both sites (Barbate, Camarinal) were very close to each other in the bidimensional space. The remaining samples, consisting of hybrid classes from the hybrid zone, showed considerable variability, mainly along PC1.

The evolutionary relationships identified in the Neighbour-Net analysis were consistent with the PCA results. The WD network showed *A. pungens* from Trafalgar far apart from all other samples, while all *A. macrophylla* from both sites clustered together (Figure 3). As with the PCA, this analysis highlighted the close genetic relatedness of individuals within the two external sites compared to individuals from Camarinal. The placement of the hybrid classes was consistent with expectations, e.g., backcrosses were close to their recurrent progenitors, F1 and F2 were in intermediate positions. Also consistent with the hybrid zone are a number of parallel edges that reflect phylogenetic uncertainty and coincide with the placement of the hybrid samples (Figure 3).

Bayesian clustering analysis of 614 unlinked SNPs from 155 samples with STRUCTURE identified $K = 2$ as the optimal partition followed by $K = 4$. Both partitions revealed substantial admixture limited to the Camarinal site (Figure 1c). The two genetic groups identified in $K = 2$ corresponded to the two species. The first group reached Q values close to 1 only in the Trafalgar site whereas the second group reached Q values close to 1 in both Barbate and Camarinal. Admixed individuals were present, with varying proportions of the two genetic groups. For $K = 4$, each of the genetic groups from $K = 2$ was split into two groups, separating Camarinal from both external populations. Seven samples from Camarinal had $Q > 0.95$ for *A. pungens* for $K = 4$ (dark grey in Figure 1c), compared to only one sample for $K = 2$, with other Camarinal individuals having varying admixture proportions.

NewHybrids analysis of the WD dataset based on 151 unlinked SNPs provided a similar but more detailed picture of the hybrid zone (Figure 1d). In the two external sites, all samples were assigned to P1 or P2 with posterior probability = 1. In Camarinal, PP > 0.95 was found in 7 samples for P1 (*A. pungens*) and in 61 samples for P2, as well as for F1 ($n = 3$), F2 ($n = 17$), BC1 ($n = 2$), or BC2 ($n = 10$). Additional hybrid samples ($n = 15$) could not be unambiguously assigned to a single genotypic class (PP < 0.95; Figure S1). Analysis of the CO dataset (115 samples based on 151 SNPs) showed a similar representation of genotypic classes: P1 ($n = 10$), BC1 ($n = 9$), F1 ($n = 7$), F2 ($n = 6$), BC2 ($n = 8$), and P2 ($n = 61$) with PP > 0.95 (Figure 1d). Fourteen additional samples had PP < 0.95. The number of samples assigned with confidence to P1 (*A. pungens*), F1, or BC1 was higher in CO than in WD, probably because the reference *A. pungens* progenitor of Camarinal is genetically closer to the genotypes found in the hybrid zone (Figure 3).

Spatially, admixed individuals were restricted to a narrow hybrid zone that runs parallel to the coastline. Its width, estimated

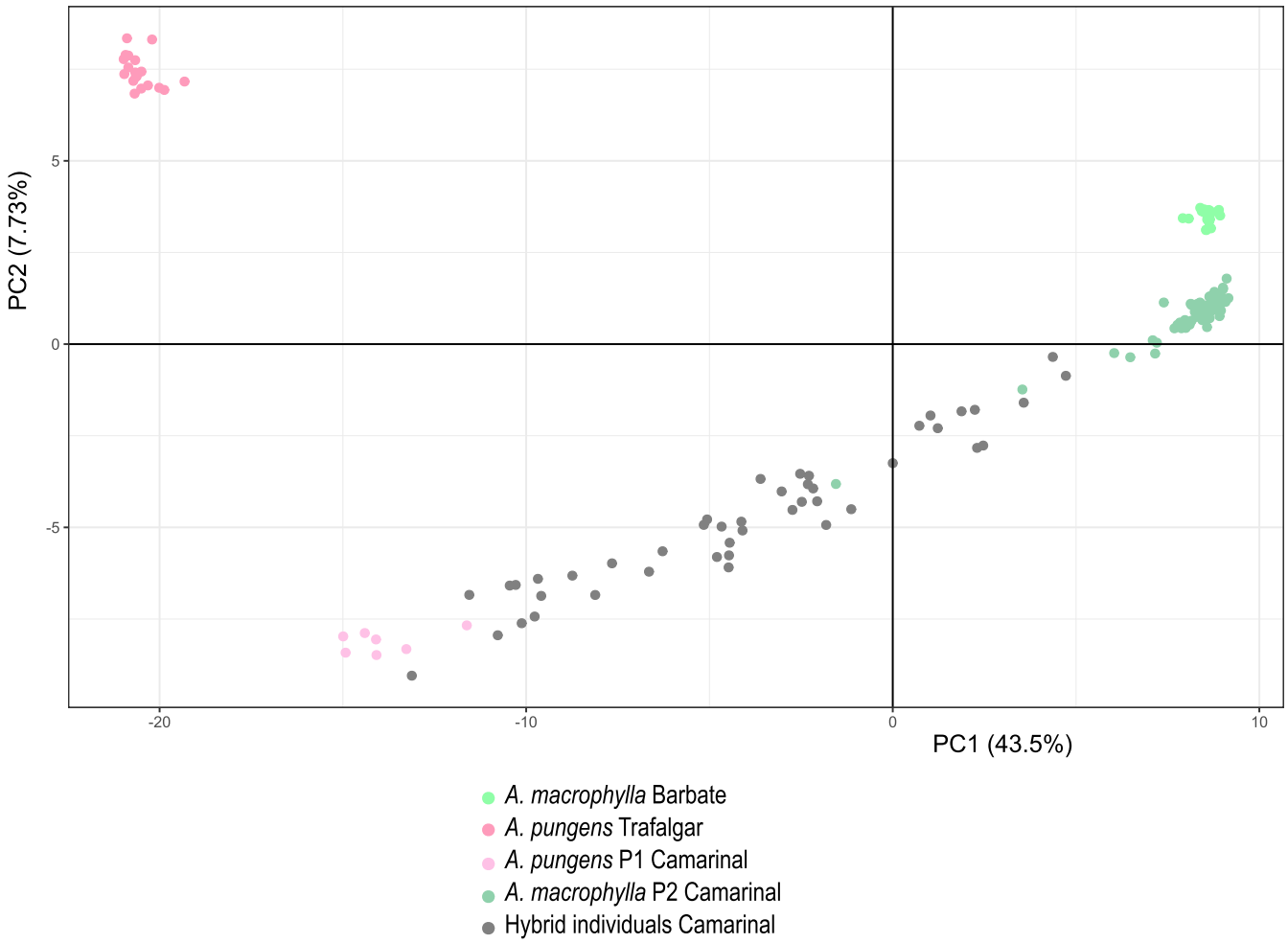

FIGURE 2 Principal component analysis of 155 *Armeria* samples based on 4412 SNPs, labelled by genotypic classes according to NewHybrids analysis of the WD dataset; the first two PCs accounted for 51.23% of the total variance (43.5% and 7.73%, respectively). Colour code represents the genotypic class to which the individual had the highest posterior probability of being assigned. Hybrid classes F1, F2, BC1 and BC2 were pooled into a single group.

considering only genotyped hybrid individuals and measured perpendicular to the coastline, is c. 18–50 m (Figure 1a).

The highest nucleotide diversity within groups was found in the hybrid group from Camarinal ($\pi = 0.053$) and the lowest in *A. pungens* population from Trafalgar ($\pi = 0.019$, Table S3). Regarding F_{ST}, the highest genetic differentiation occurred between the two external populations, Trafalgar *A. pungens* vs. Barbate *A. macrophylla* ($F_{ST} = 0.776$, Table S4). The lowest occurred between *A. pungens* P1 from Camarinal and the hybrid group from that site ($F_{ST} = 0.167$). When considering the F_{ST} between allopatric populations of the same species, the F_{ST} between the Trafalgar and Camarinal sites of *A. pungens* was higher ($F_{ST} = 0.452$) than that between the Barbate and Camarinal sites of *A. macrophylla* ($F_{ST} = 0.176$, Table S4). The group containing all hybrid classes showed the highest expected heterozygosity ($H_e = 0.148$), followed by *A. pungens* from Camarinal (0.084) and *A. macrophylla* from Camarinal ($H_e = 0.082$, Table S3). The lowest heterozygosity was found in the populations of *A. pungens* from Trafalgar ($H_e = 0.049$) and *A. macrophylla* from Barbate ($H_e = 0.075$).

3.4 | Genomic introgression

Genomic cline analyses of WD based on 553 SNPs, i.e., one SNP per locus with MAF > 0.05, yielded hybrid indices between 0.228 and 0.919 for samples from Camarinal (Figure S7). For α, there was considerable variability across loci, indicating rather different proportions of P1 and P2 ancestries depending on the locus. Outliers for α ($n = 171$) included 116 loci with excess *A. pungens* ancestry ($-4.248 \leq \alpha \leq -0.827$) and 55 with excess *A. macrophylla* ancestry ($1.789 \leq \alpha \leq 4.330$, Table S5). With respect to β, genomic clines for several loci were steep, suggesting limited introgression between *A. pungens* and *A. macrophylla* (e.g., locus 23,710, $\beta = 1.353$, Table S5), whereas higher rates of introgression were detected for other loci (e.g., locus 27,539, $\beta = -1.438$, Table S5). Four loci were identified as β outliers. All had negative values for this parameter in the admixed population (−0.868 to −0.757), consistent with wider than expected genomic clines and thus a gradual change in allele frequencies between *A. pungens* and *A. macrophylla* (Table S5). Restricting the genomic cline analysis to

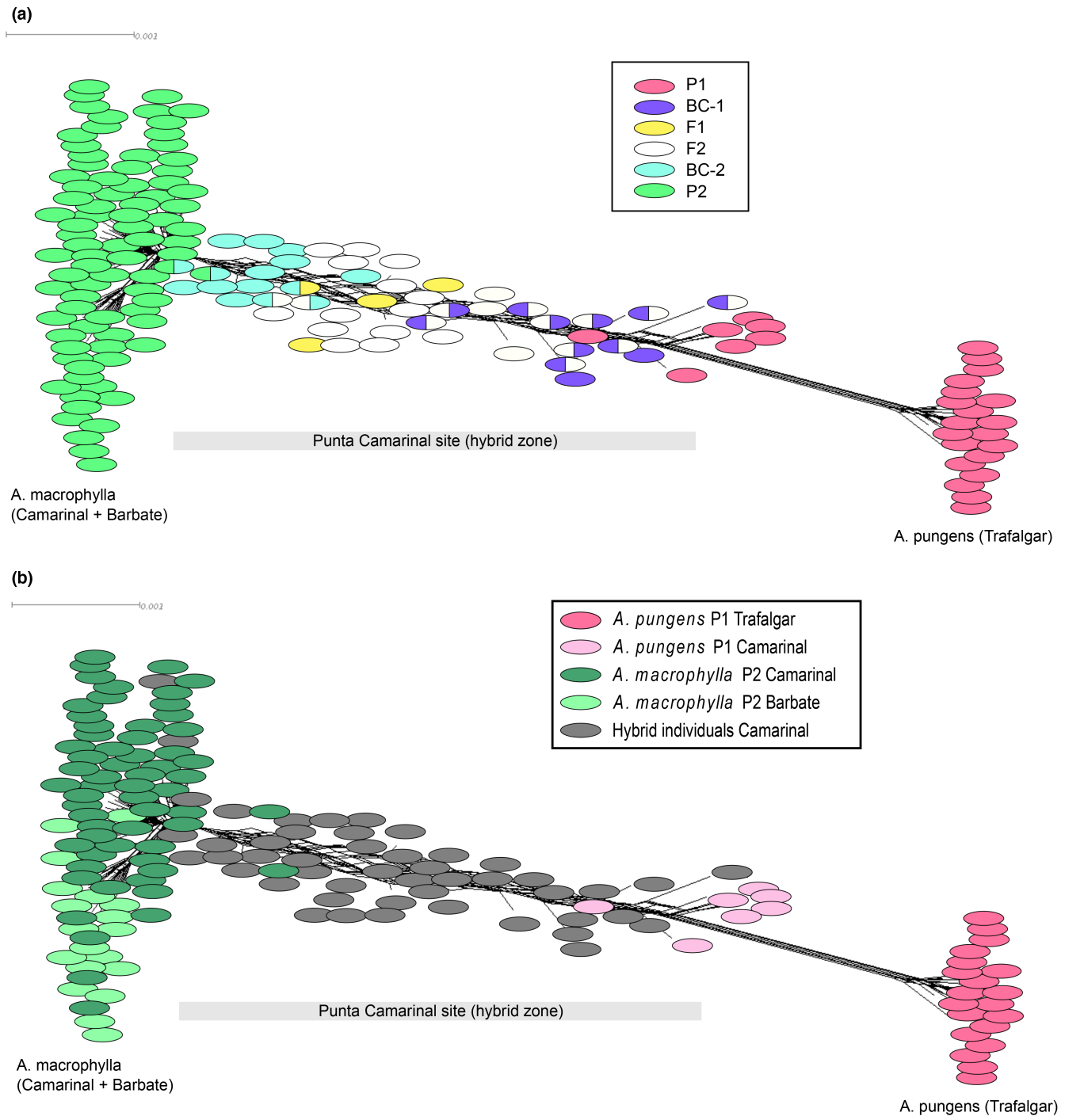

FIGURE 3 Neighbour-Net diagram showing relationships among 155 *Armeria* samples based on 4412 SNPs. Colour-code follows NewHybrids genotypic classes. (a) In admixed samples with PP <0.95 of belonging to one of the genotypic classes, two are shown, the left one corresponding to the class with the highest posterior probability. (b) Genotypic class shown for each individual is that with the highest PP, as in Figure 2, with hybrid classes F1, F2, BC1 and BC2 pooled into a single group and samples from the external populations specifically labelled.

Camarinal (CO dataset) and the same 553 sampled loci resulted in hybrid indices between 0.089 and 0.812 (Figure S8). Compared to WD, for both parameters but especially for β, the range of values for each locus across samples was narrow and homogeneous, likely because the progenitors used in this dataset are genetically closer to the genotypes found in the hybrid zone. Four loci were identified as α outliers in the admixed population, all indicating an excess of *A. pungens* ancestry. No outliers were identified for β (Table S6).

Tests for non-recent introgression resulted in an excess of the ABBA pattern for both scenarios, indicating introgression between *A. macrophylla* and *A. pungens* from the Camarinal site. Specifically,

for the first scenario, all 60 tests were significant, whereas for the second scenario, 32 out of 60 (53.3%) were significant, identified by *Z*-scores ≥ 2.58 (Table S7). The *D*-statistic values ranged from 0.34 to 0.59 for the first scenario, and from 0.04 to 0.45 for the second. On average, 532.1 loci were used per test.

3.5 | Demographic history

Effective population size (N_e) over time based on 1271 linkage-pruned but not MAF-filtered SNPs, visualized in Stairway plots, did not show dramatic changes in any of the four non-introgressed populations; old expansions (between 200,000 and 20,000 years ago) occurred in all groups, showing similar demographic patterns (Figure S9). The most probable demographic scenario involving all four gene pools, as inferred by Fastsimcoal2, was model 4, which included gene flow between the *A. pungens* and *A. macrophylla* populations from the Camarinal site since the divergence of the two *A. pungens* populations (Figure 4). This model had the highest likelihood as well as the best AIC value of the four models that included four gene pools (Table 1). Confidence intervals for parameter estimates in this model failed to include some of the parameter point estimates despite performing 50% more simulations than recommended (Table S8). According to this model, the split between the two *A. pungens* populations is estimated to have occurred during the Holocene c. 1842 (95% CI: 1939.18–2070.91) generations ago (Table S8). The split between the two *A. macrophylla* populations is estimated to have occurred c. 82 (95% CI: 315.78–350.14) generations ago whereas the split between the two species may have occurred c. 6433 (95% CI: 6267.65–6465.34) generations ago. Estimates of population size (N_e) range from 107 (95% CI: 395.24–436.51) for *A. macrophylla* from Barbate to 23,641 (95% CI: 23,271.00–25,023.34) for *A. pungens* from Trafalgar, with $N_e = 501$ (95% CI: 461.55–500.28) for *A. pungens* from Camarinal and $N_e = 2504$ (95% CI: 10,992.40–12,574.29) for *A. macrophylla* from Camarinal with between. At the Camarinal site, Fastsimcoal migration rates indicated that any gene copy in *A. pungens* had a probability of 2.20e-05 of being a migrant from *A. macrophylla*, whereas any gene copy in *A. macrophylla* had a probability of 3.38e-04 of being a migrant from *A. pungens*. These estimates are small overall, but suggest a higher rate of forward migration toward *A. macrophylla* (Table S8).

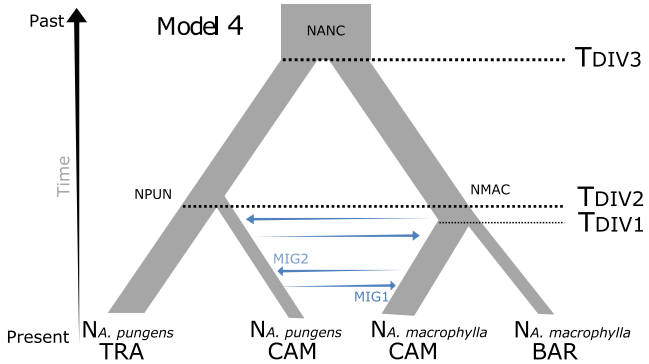

FIGURE 4 Best demographic model for the history of the studied hybrid zone inferred with Fastsimcoal2 (Excoffier et al., 2013) using four groups (progenitors from Camarinal site and external populations), and excluding hybrids as identified by NewHybrids (WD dataset). *N*, effective population size; TDIV1, TDIV2, TDIV3, divergence times; MIG1, MIG2, migration rates. See Table S8 for point estimate values for these parameters.

3.6 | Plastid genome analysis

A total of thirty-five scaffolds were identified from the *A. pungens* plastid genome. After assembly, filtering and imputation of missing data, 41 SNPs were recovered from the ddRADseq data in 158 samples. Thirty-four haplotypes were identified, a large number of which (21 haplotypes) were singletons occurring in 11 individuals from the Camarinal site, six in *A. pungens* from Trafalgar, and four in *A. macrophylla* from Barbate (Figure S10, Table S9). Three frequent haplotypes were shared among species and genotypic classes. One (# 7) occurred in 58 samples from Camarinal from all genotypic classes and in one sample from the geographically close population of *A. hirta*; the second most frequent haplotype (# 9) occurred in 31 samples from Camarinal and in one sample of *A. pungens* from Trafalgar. The third (# 3) occurred in 11 *A. macrophylla* from Barbate, in six *A. pungens* from Trafalgar and in the other two samples of *A. hirta*. The haplotype distribution shows a clear geographical structure, where all twenty haplotypes detected in Camarinal are not found elsewhere, with two exceptions, for # 7 (one individual of 59 carrying this haplotype) and # 9 (one of 33; Table S9).

4 | DISCUSSION

This study highlights the difficulty of integrating results of multiple analyses of hybrid zones to derive evolutionary processes within syngameons, especially when the drivers of bidirectional introgression differ in each direction. This complexity is exacerbated in non-model systems where it is difficult to integrate empirical observations with

TABLE 1 Likelihood and Akaike information criterion (AIC) values for demographic models selection tested with Fastsimcoal2.

Model	Log likelihood	deltaL	AIC	ΔAIC
Model 1	−1613.92	101.097	3718.187	[a]
Model 2	−9526.90	515.31	43894.98	−175.16
Model 3	−9517.48	505.89	43855.61	−135.79
Model 4	−9487.99	476.40	43719.82	0.00
Model 5	−9501.34	489.75	43783.28	−63.46

Note: See text and Figure S4 for description of scenarios.

[a]Note that model 1 involves two genetic pools whereas 2–5 involve four. Model 1 is poorly informative for reconstructing the demographic history of the hybrid zone and comparison with the other four is not meaningful.

theory (Butlin & Ritchie, 2013; Edwards et al., 2016; Nieto Feliner et al., 2017, 2020; Sætre, 2013). Using multiple lines of evidence is crucial for reconstructing complex evolutionary scenarios in such systems (Cruzan et al., 2021; Janzen et al., 2019; Ortego et al., 2018; Zhang et al., 2022; this study). Determining the genetic structure and inferring the demographic history of populations, performing genomic cline analysis and introgression tests, and examining associations between habitat, phenotypes and genetic groups, have all revealed pertinent insights into the history and drivers of the hybrid zone under investigation. Our analyses shed light on the discrepancies between phenotypic and genomic patterns in the hybrid zone and the causes of the genetic distinctiveness of the peripheral *A. pungens* population. This distinctiveness is due to recent and non-recent introgression, as well as to divergence resulting from isolation and genetic drift. Our study also revealed ancient introgression between the two species and that there are twice as many outlier loci with excess *A. pungens* ancestry than loci with excess *A. macrophylla* ancestry. Despite these significant findings in the system, some questions on the evolutionary processes remain unanswered.

4.1 | Plastid introgression and capture

Organellar DNA loci are critical alongside nuclear loci to interpret complex introgression scenarios, as they can elucidate processes that differentially affect both genomic compartments, such as different dispersal via pollen or seeds (Petit & Excoffier, 2009). Plastid capture has been inferred in systems that display a geographic rather than a taxonomic pattern of plastid variation (Acosta & Premoli, 2010; Boom et al., 2021; Chen et al., 2022; Folk et al., 2017; Vitelli et al., 2017). A possible factor contributing to plastid introgression in certain species could be selection (Lee-Yaw et al., 2019). Selection has been attributed a role in the sole theoretical model currently available for plastid capture (Tsitrone et al., 2003). However, the prevailing view that plastid variation is largely neutral has not been seriously challenged (Bock et al., 2014). Under non-adaptive plastid variation, demographic factors should drive plastid introgression and capture. This is supported in Currat et al.'s (2008) model for invasion scenarios, where an initial demographic imbalance between the invading and resident populations leads to massive introgression of the invader by the local population.

Assuming that there is no selection pressure on plastid variation, it is possible that there was a plastid capture at our study site, which aligns with the scenario presented by Currat et al. (2008). Abundance of habitat suitable for *A. macrophylla* and a larger estimated Ne in this species suggest that in Camarinal, *A. macrophylla* was the original species while a few *A. pungens* founders arrived later and captured the local *A. macrophylla* plastome. This process was likely driven by a demographic imbalance in the early stages of *A. pungens* colonization, pollination of *A. macrophylla* by *A. pungens*, and backcrossing to *A. pungens* in dune environments. Furthermore, previous Sanger sequencing data focusing on non-coding plastid regions throughout the *A. pungens* range identified a haplotype private to the Camarinal site (Piñeiro et al., 2011). Our observations of bidirectional introgression at nuclear loci and an enrichment of outlier loci with *A. pungens* ancestry in this site with harsh environmental conditions are consistent with theory in which loci under strong positive selection in *A. pungens* have resisted introgression (Kane et al., 2009; Parchman et al., 2013).

Plastid sharing patterns observed outside of the study site, specifically between *A. pungens* from Trafalgar and *A. macrophylla* from Barbate, could be attributed to ancient sharing of ancestral haplotypes (haplotypes #3 and #4), as these two species share Sanger sequencing-based haplotypes along the Gulf of Cadiz (Nieto Feliner et al., 2019). Thus, extensive haplotype sharing across species and genotypic classes highlights a clear geographic signal for plastid DNA variation, which is consistent with introgression and plastid capture.

4.2 | Different introgression drivers for the two hybridizing species

Our study provides a microevolutionary perspective that complements previous macroevolutionary studies in the *Armeria* syngameon (see Introduction) and may help to understand how hybridizing species interact within other syngameons. Our proposed microevolutionary scenario can be summarized as follows: (1) Sp1 (in our study, *A. pungens*) typical of a challenging environment (e.g., high solar radiation, saline influence, and deep sandy soils) disperses to a peripheral location where it suffers low effective population size, Ne, due to the founder event. (2) The Ne of Sp1 increases because of introgression from an abundant congener, Sp2 (*A. macrophylla*), that occurs in an adjacent less challenging environment (e.g., pinewood or macchia shrubland understory), belongs to the same syngameon, shares generalist pollinators, and has the same self-incompatibility system. (3) Adaptive alleles from Sp1 facilitate the survival of introgressed Sp2 individuals in harsher environments.

Evidence for beneficial effects of introgression is accumulating for a variety of organisms and evolutionary scenarios (Hübner et al., 2019; Leroy et al., 2020; Mostert-O'Neill et al., 2021; Wang et al., 2019), including for bottlenecks resulting from colonization events (Besnard et al., 2014). The peripheral *A. pungens* population in our study is also consistent with a commonly reported consequence of introgression —range and/or niche expansion and survival at range edges (Chhatre et al., 2018; Pfennig et al., 2016)—, which may have been important in postglacial colonization scenarios (Kremer & Hipp, 2020; Petit et al., 2004). At the northern range edge of *A. pungens*, on an offshore island located hundreds of kilometres away from the nearest conspecific population, this species forms another hybrid zone with *A. pubigera* (Piñeiro et al., 2011). The two recognized hybrid zones in which *A. pungens* is involved illustrate the tendency of species within syngameons to hybridize at the range edges.

Our proposed scenario fits all the evidence, with a few caveats. A search for outlier loci using the most stringent selection method indicates that those enriched in *A. pungens* ancestry are twice

as frequent as those enriched in *A. macrophylla* ancestry. While not all of these outliers are necessarily products of selection, it is likely that some are (Gompert & Buerkle, 2011) and follow the same enrichment proportions. However, annotation of these loci did not identify specific candidates that aid survival under harsh conditions, except for one related to beta-galactosidase, which is associated with organ growth and matches a greater biomass in *A. pungens* compared to *A. macrophylla*. This could be due to the use of a reduced representation genomic approach, ddRADseq, and the polygenic nature of traits coping with environment (Leroy et al., 2020). Another caveat is that we did not estimate fitness or analyse Bateson–Dobzhansky–Muller incompatibilities in hybrid classes, both of which are beyond the scope of this study. However, we do have indirect evidence from 36 healthy synthetic hybrids — obtained from crosses between three populations (*A. pungens* and *A. macrophylla* from Camarinal, and *A. pungens* from Trafalgar) — and grown for years under greenhouse conditions (Nieto Feliner et al., 2019). A third caveat is the difficulty in estimating confidence intervals for the parameters of the best demographic model. This may suggest that the scenarios we tested are complex and involve many parameters, and that in our attempt to infer non-recent gene flow by selecting pure individuals, we may have assumed as pure some samples that are actually introgressed. Past gene flow is supported by our ABBA-BABA tests, and by the best demographic model inferred from the data, which includes gene flow since the split of the two *A. pungens* populations. The difficulties in estimating parameter confidence intervals in this model, possibly due in part to old unaccounted gene flow, highlight the caution that should be taken when performing coalescence modelling in syngameons.

Even with these caveats, the best interpretation of the available data from this hybrid zone is that the peripheral population of *A. pungens* experiences gene flow with *A. macrophylla* avoiding reduced levels of genetic diversity due to its small size and isolated location, and ensuing demographic risks, and *A. macrophylla* is expanding its niche into open harsh habitats thanks to adaptive introgression.

4.3 | Prospects

Predicting the medium- and long-term consequences of the current scenario is relevant to our overarching goal of linking early stages of hybridization with the currently observed diversity in *Armeria*, which is partly the result of ancient hybridization, i.e., linking recent with ancient hybridization in this genus. However, the long-term consequences will depend on the interaction of several factors. If *A. macrophylla* continues to colonize open habitats through hybridization with *A. pungens*, in the long run there will be an introgressed population that will look more like *A. macrophylla* than it does now. Whether this projection involves the genetic assimilation of *A. pungens* into *A. macrophylla* (swamping of *A. pungens*) depends on how large and genetically isolated the Camarinal population of *A. pungens* will remain. *A. pungens* may have long resisted this swamping, conserving typical *A. pungens* morphological traits in pure samples near the coastline despite long-lasting interspecific gene flow (for 1842 generations according to our simulations) and possible plastid capture (of *A. macrophylla* plastome). A possible explanation for this resistance to swamping is the harsh environmental conditions in which *A. pungens* grows. Another factor could be the presence of recombination cold spots, inversions or chromosomal rearrangements that prevent introgression from *A. macrophylla* (Huang & Rieseberg, 2020), and if true, *A. pungens* could persist at this site in the future. Another factor to consider is whether the planting of a pinewood c. 60 years ago has altered the dynamics of this hybrid zone by extending the contact between the habitats of the two species.

Our inference of these possible bidirectional beneficial effects of introgression is relevant in the context of the evolutionary dynamics of syngameons as networks that are 'more than the sum of their parts' (Cannon & Petit, 2020). Although bidirectional introgression has been reported in various contexts (Brubaker et al., 1993; Marburger et al., 2019), reported cases typically focus on the directionality of benefits to one of the hybridizing species.

We consider that the scenario inferred here should be considered when studying interactions between species within a syngameon. Given the abundant evidence of ancient hybridization in the *Armeria* syngameon based on macroevolutionary approaches (Fuertes et al., 1999a; Fuertes & Nieto Feliner, 2003), we also highlight the dynamic nature of syngameons over evolutionary time (Cronk & Suarez-Gonzalez, 2018).

AUTHOR CONTRIBUTIONS

GNF designed the study with suggestions by IVM and MH. IA, IVM and GNF sampled materials. IVM conducted lab work and data analysis, and MH hosted IVM at INRAE and advised on data analysis. All authors interpreted results. IVM and GNF wrote the first draft of the manuscript, and all authors revised the manuscript and approved the final version.

ACKNOWLEDGEMENTS

The authors thank Jonathan Wendel and Josep A. Rosselló for useful comments and discussion, Mitch Cruzan, Vikram Chhatre and three anonymous reviewers for their very constructive suggestions, José L. Blanco-Pastor for his suggestions on modelling, Laura Barrios for her help in statistical analyses, David Criado for his help in ABBA-BABA analysis, Alberto Herrero for DNA extraction and quality assessment, Juan Arroyo for information on the Barbate population, the Spanish Ministry of Defence for granting permission to sample in the Camarinal site, located within the Acuartelamiento el Bujeo, and specifically to Francisco Cebrián for providing information on vegetation changes during the 20th century. This work has benefited from support of Spanish Ministry of Science and Innovation-Spanish Agency for Investigation, Grant CGL2017-88500-P (AEI/FEDER, UE) to GNF and a LabEx COTE Fellowship (Laboratoire d'Excellence, Université de Bordeaux) to IVM. This work has benefited from support of a grant from Investissement d'Avenir grants of the ANR (CEBA:ANR-10-LABX-25-01) to MH. We also acknowledge support

of the publication fee by the CSIC Open Access Publication Support Initiative through its Unit of Information Resources for Research (URICI).

CONFLICT OF INTEREST STATEMENT

The authors declared no conflict of interest for this article.

DATA AVAILABILITY STATEMENT

Raw ddRADseq reads have been deposited at the Sequence Read Archive (SRA) through the NCBI BioProject PRJNA971618 (https://www.ncbi.nlm.nih.gov/sra/PRJNA971618; Table S10). SNPs datasets and plastid sequences of *Armeria pungens* are available in the institutional repository DIGITAL CSIC (https://doi.org/10.20350/digitalCSIC/15290). Scripts of several analyses (PCA, genomic cline and chloroplast SNP calling) are available on GitHub (https://github.com/Irvilma/hybrid_zone_armeria/tree/main).

ORCID

Irene Villa-Machío https://orcid.org/0000-0002-4281-5975
Gonzalo Nieto Feliner https://orcid.org/0000-0002-7469-4733

REFERENCES

Abbott, R. J., Barton, N. H., & Good, J. M. (2016). Genomics of hybridization and its evolutionary consequences. *Molecular Ecology*, *25*(11), 2325–2332. https://doi.org/10.1111/mec.13685

Acosta, M. C., & Premoli, A. C. (2010). Evidence of chloroplast capture in south American *Nothofagus* (subgenus Nothofagus, Nothofagaceae). *Molecular Phylogenetics and Evolution*, *54*(1), 235–242. https://doi.org/10.1016/j.ympev.2009.08.008

Anderson, E. (1949). *Introgressive hybridization*. John Wiley.

Anderson, E. C., & Thompson, E. A. (2002). A model-based method for identifying species hybrids using multilocus genetic data. *Genetics*, *160*(3), 1217–1229. https://doi.org/10.1093/genetics/160.3.1217

Andrews, S. (2010). FastQC: A quality control tool for high throughput sequence data.

Arnold, M. L., Bouck, A. C., & Scott Cornman, R. (2004). Verne Grant and Louisiana irises: Is there anything new under the sun? *New Phytologist*, *161*(1), 143–149. https://doi.org/10.1046/j.1469-8137.2003.00856.x

Baker, H. G. (1966). The evolution, functioning and breakdown of heteromorphic incompatibility systems. I. The Plumbaginaceae. *Evolution*, *20*, 349–368. https://doi.org/10.2307/2406635

Bankevich, A., Nurk, S., Antipov, D., Gurevich, A. A., Dvorkin, M., Kulikov, A. S., Lesin, V. M., Nikolenko, S. I., Pham, S., Prjibelski, A. D., Pyshkin, A. V., Sirotkin, A. V., Vyahhi, N., Tesler, G., Alekseyev, M. A., & Pevzner, P. A. (2012). SPAdes: A new genome assembly algorithm and its applications to single-cell sequencing. *Journal of Computational Biology*, *19*(5), 455–477. https://doi.org/10.1089/cmb.2012.0021

Baumel, A., Médail, F., Juin, M., Paquier, T., Clares, M., Laffargue, P., Lutard, H., Dixon, L., & Pires, M. (2020). Population genetic structure and management perspectives for *Armeria belgenciencis*, a narrow endemic plant from Provence (France). *Plant Ecology and Evolution*, *153*(2), 219–228. https://doi.org/10.5091/plecevo.2020.1702

Besnard, G., Dupuy, J., Larter, M., Cuneo, P., Cooke, D., & Chikhi, L. (2014). History of the invasive African olive tree in Australia and Hawaii: Evidence for sequential bottlenecks and hybridization with the Mediterranean olive. *Evolutionary Applications*, *7*(2), 195–211. https://doi.org/10.1111/eva.12110

Bock, D. G., Andrew, R. L., & Rieseberg, L. H. (2014). On the adaptive value of cytoplasmic genomes in plants. *Molecular Ecology*, *23*(20), 4899–4911. https://doi.org/10.1111/mec.12920

Boecklen, W. J. (2017). Topology of Syngameons. *Ecology and Evolution*, *7*(24), 10486–10491. https://doi.org/10.1002/ece3.3507

Bog, M., Ehrnsberger, H. F., Elmer, M., Bässler, C., & Oberprieler, C. (2017). Do differences in herbivore resistance contribute to elevational niches of species and hybrids in the central European *Senecio nemorensis* (Compositae, Senecioneae) syngameon? *Perspectives in Plant Ecology, Evolution and Systematics*, *24*, 61–71. https://doi.org/10.1016/j.ppees.2016.12.003

Bolger, A. M., Lohse, M., & Usadel, B. (2014). Trimmomatic: A flexible trimmer for Illumina sequence data. *Bioinformatics*, *30*(15), 2114–2120. https://doi.org/10.1093/bioinformatics/btu170

Boom, A. F., Migliore, J., Kaymak, E., Meerts, P., & Hardy, O. J. (2021). Plastid introgression and evolution of African miombo woodlands: New insights from the plastome-based phylogeny of *Brachystegia* trees. *Journal of Biogeography*, *48*(4), 933–946. https://doi.org/10.1111/jbi.14051

Browning, S. R., & Browning, B. L. (2007). Rapid and accurate haplotype phasing and missing-data inference for whole-genome association studies by use of localized haplotype clustering. *The American Journal of Human Genetics*, *81*(5), 1084–1097. https://doi.org/10.1086/521987

Brubaker, C. L., Koontz, J. A., & Wendel, J. F. (1993). Bidirectional cytoplasmic and nuclear introgression in the New World cottons *Gossypium barbadense* and *G. Hirsutum* (Malvaceae). *American Journal of Botany*, *80*(10), 1203–1208. https://doi.org/10.1002/j.1537-2197.1993.tb15353.x

Butlin, R. K., & Ritchie, M. G. (2013). Pulling together or pulling apart: Hybridization in theory and practice. *Journal of Evolutionary Biology*, *26*, 294–298. https://doi.org/10.1111/jeb.12080

Camacho, C., Coulouris, G., Avagyan, V., Ma, N., Papadopoulos, J., Bealer, K., & Madden, T. L. (2009). BLAST+: Architecture and applications. *BMC Bioinformatics*, *10*, 421. https://doi.org/10.1186/1471-2105-10-421

Cannon, C. H., & Lerdau, M. (2015). Variable mating behaviors and the maintenance of tropical biodiversity. *Frontiers in Genetics*, *6*, 183. https://doi.org/10.3389/fgene.2015.00183

Cannon, C. H., & Lerdau, M. T. (2019). Demography and destiny: The syngameon in hyperdiverse systems. *Proceedings of the National Academy of Sciences*, *116*(17), 8105. https://doi.org/10.1073/pnas.1902040116

Cannon, C. H., & Petit, R. J. (2020). The oak syngameon: More than the sum of its parts. *New Phytologist*, *226*(4), 978–983. https://doi.org/10.1111/nph.16091

Caujapé-Castells, J., García-Verdugo, C., Marrero-Rodríguez, Á., Fernández-Palacios, J. M., Crawford, D. J., & Mort, M. E. (2017). Island ontogenies, syngameons, and the origins and evolution of genetic diversity in the Canarian endemic flora. *Perspectives in Plant Ecology, Evolution and Systematics*, *27*, 9–22. https://doi.org/10.1016/j.ppees.2017.03.003

Chen, S., Milne, R., Zhou, R., Meng, K., Yin, Q., Guo, W., Ma, Y., Mao, K., Xu, K., Kim, Y.-D., Van Do, T., Liao, W., & Fan, Q. (2022). When tropical and subtropical congeners met: Multiple ancient hybridization events within *Eriobotrya* in the Yunnan-Guizhou plateau, a tropical-subtropical transition area in China. *Molecular Ecology*, *31*(5), 1543–1561. https://doi.org/10.1111/mec.16325

Chhatre, V. E., Evans, L. M., DiFazio, S. P., & Keller, S. R. (2018). Adaptive introgression and maintenance of a trispecies hybrid complex in range-edge populations of *Populus*. *Molecular Ecology*, *27*(23), 4820–4838. https://doi.org/10.1111/mec.14820

Cronk, Q. C., & Suarez-Gonzalez, A. (2018). The role of interspecific hybridization in adaptive potential at range margins. *Molecular Ecology*, *27*, 4653–4656. https://doi.org/10.1111/mec.14927

Cruzan, M. B., Thompson, P. G., Diaz, N. A., Hendrickson, E. C., Gerloff, K. R., Kline, K. A., Machiorlete, H. M., & Persinger, J. M. (2021). Weak coupling among barrier loci and waves of neutral and adaptive introgression across an expanding hybrid zone. *Evolution*, *75*, 3098–3114. https://doi.org/10.1111/evo.14381

Currat, M., Ruedi, M., Petit, R. J., & Excoffier, L. (2008). The hidden side of invasions: Massive introgression by local genes. *Evolution*, *62*(8), 1908–1920. https://doi.org/10.1111/j.1558-5646.2008.00413.x

Danecek, P., Auton, A., Abecasis, G., Albers, C. A., Banks, E., DePristo, M. A., Handsaker, R. E., Lunter, G., Marth, G. T., Sherry, S. T., Mcvean, G., Durbin, R., & 1000 Genomes Project Analysis Group. (2011). The variant call format and VCFtools. *Bioinformatics*, *27*(15), 2156–2158. https://doi.org/10.1093/bioinformatics/btr330

De La Torre, A. R., Li, Z., Van de Peer, Y., & Ingvarsson, P. K. (2017). Contrasting rates of molecular evolution and patterns of selection among gymnosperms and flowering plants. *Molecular Biology and Evolution*, *34*(6), 1363–1377. https://doi.org/10.1093/molbev/msx069

Doyle, J. J., & Doyle, J. L. (1987). A rapid DNA isolation procedure for small quantities of fresh leaf tissue. *Phytochemical Bulletin*, *19*, 11–15.

Durand, E. Y., Patterson, N., Reich, D., & Slatkin, M. (2011). Testing for ancient admixture between closely related populations. *Molecular Biology and Evolution*, *28*, 2239–2252. https://doi.org/10.1093/molbev/msr048

Earl, D. A. (2012). STRUCTURE HARVESTER: A website and program for visualizing STRUCTURE output and implementing the Evanno method. *Conservation Genetics Resources*, *4*(2), 359–361. https://doi.org/10.1007/s12686-011-9548-7

Eaton, D. A. R. (2014). PyRAD: Assembly of de novo RADseq loci for phylogenetic analyses. *Bioinformatics*, *30*, 1844–1849. https://doi.org/10.1093/bioinformatics/btu121

Eaton, D. A. R., & Overcast, I. (2020). Ipyrad: Interactive assembly and analysis of RADseq datasets. *Bioinformatics*, *36*(8), 2592–2594. https://doi.org/10.1093/bioinformatics/btz966

Eaton, D. A. R., & Ree, R. H. (2013). Inferring phylogeny and introgression using RADseq data: An example from flowering plants (*Pedicularis*: Orobanchaceae). *Systematic Biology*, *62*, 689–706. https://doi.org/10.1093/sysbio/syt032

Edwards, S. V., Potter, S., Schmitt, C. J., Bragg, J. G., & Moritz, C. (2016). Reticulation, divergence, and the phylogeography–phylogenetics continuum. *Proceedings of the National Academy of Sciences*, *113*(29), 8025–8032. https://doi.org/10.1073/pnas.1601066113

Evanno, G., Regnaut, S., & Goudet, J. (2005). Detecting the number of clusters of individuals using the software STRUCTURE: A simulation study. *Molecular Ecology*, *14*(8), 2611–2620. https://doi.org/10.1111/j.1365-294X.2005.02553.x

Excoffier, L., Dupanloup, I., Huerta-Sánchez, E., Sousa, V. C., & Foll, M. (2013). Robust demographic inference from genomic and SNP data. *PLoS Genetics*, *9*(10), e1003905. https://doi.org/10.1371/journal.pgen.1003905

Folk, R. A., Mandel, J. R., & Freudenstein, J. V. (2017). Ancestral gene flow and parallel organellar genome capture result in extreme phylogenomic discord in a lineage of angiosperms. *Systematic Biology*, *66*(3), 320–337. https://doi.org/10.1093/sysbio/syw083

Fuertes, J., & Nieto Feliner, G. (2003). Additive polymorphisms and reticulation in an ITS phylogeny of thrifts (*Armeria*, Plumbaginaceae). *Molecular Phylogenetics and Evolution*, *28*(3), 430–447. https://doi.org/10.1016/S1055-7903(02)00301-9

Fuertes, J., Rosselló, J. A., & Nieto Feliner, G. (1999a). Molecular evidence for the compilospecies model of reticulate evolution in *Armeria* (Plumbaginaceae). *Systematic Biology*, *48*(4), 735–754. https://doi.org/10.1080/106351599259997

Fuertes, J., Rosselló, J. A., & Nieto Feliner, G. (1999b). Nuclear ribosomal DNA (nrDNA) concerted evolution in natural and artificial hybrids of *Armeria* (Plumbaginaceae). *Molecular Ecology*, *8*(8), 1341–1346. https://doi.org/10.1046/j.1365-294X.1999.00690.x

García-Camacho, R., Méndez, M., & Escudero, A. (2009). Pollination context effects in the high-mountain dimorphic *Armeria caespitosa* (Plumbaginaceae): Neighborhood is something more than density. *American Journal of Botany*, *96*, 1620–1626. https://doi.org/10.3732/ajb.0800374

Gompert, Z., & Buerkle, C. A. (2011). Bayesian estimation of genomic clines. *Molecular Ecology*, *20*(10), 2111–2127. https://doi.org/10.1111/j.1365-294X.2011.05074.x

Grant, V. (1981). *Plant speciation* (2nd ed.). Columbia University Press.

Gruber, B., Unmack, P. J., Berry, O. F., & Georges, A. (2018). Dartr: An r package to facilitate analysis of SNP data generated from reduced representation genome sequencing. *Molecular Ecology Resources*, *18*(3), 691–699. https://doi.org/10.1111/1755-0998.12745

Gurevich, A., Saveliev, V., Vyahhi, N., & Tesler, G. (2013). QUAST: Quality assessment tool for genome assemblies. *Bioinformatics*, *29*(8), 1072–1075. https://doi.org/10.1093/bioinformatics/btt086

Gutiérrez Larena, B., Fuertes Aguilar, J., & Nieto Feliner, G. (2002). Glacial-induced altitudinal migrations in *Armeria* (Plumbaginaceae) inferred from patterns of chloroplast DNA haplotype sharing. *Molecular Ecology*, *11*(10), 1965–1974. https://doi.org/10.1046/j.1365-294X.2002.01594.x

Hamlin, J. A., Hibbins, M. S., & Moyle, L. C. (2020). Assessing biological factors affecting postspeciation introgression. *Evolution Letters*, *4*(2), 137–154. https://doi.org/10.1002/evl3.159

Harlan, J. R., & De Wet, J. M. J. (1963). The compilospecies concept. *Evolution*, *17*, 497–501. https://doi.org/10.2307/2407101

Heiser, C. B. (1973). Introgression reexamined. *Botanical Review*, *39*(4), 347–366. https://doi.org/10.1007/BF02859160

Herrera, J. (1987). Flower and fruit biology in southern Spanish Mediterranean shrublands. *Annals of the Missouri Botanical Garden*, *74*, 69–78. https://doi.org/10.2307/2399263

Hibbins, M. S., & Hahn, M. W. (2022). Phylogenomic approaches to detecting and characterizing introgression. *Genetics*, *220*(2), iyab173. https://doi.org/10.1093/genetics/iyab173

Huang, K., & Rieseberg, L. H. (2020). Frequency, origins, and evolutionary role of chromosomal inversions in plants. *Frontiers in Plant Science*, *11*, 296. https://doi.org/10.3389/fpls.2020.00296

Hübner, S., Bercovich, N., Todesco, M., Mandel, J. R., Odenheimer, J., Ziegler, E., Lee, J. S., Baute, G. J., Owens, G. L., Grassa, C. J., Ebert, D. P., Ostevik, K. L., Moyers, B. T., Yakimowski, S., Masalia, R. R., Gao, L., Ćalić, I., Bowers, J. E., Kane, N. C., … Rieseberg, L. H. (2019). Sunflower pan-genome analysis shows that hybridization altered gene content and disease resistance. *Nature Plants*, *5*(1), 54–62. https://doi.org/10.1038/s41477-018-0329-0

Huson, D. H., & Bryant, D. (2006). Application of phylogenetic networks in evolutionary studies. *Molecular Biology and Evolution*, *23*(2), 254–267. https://doi.org/10.1093/molbev/msj030

Janzen, G. M., Wang, L., & Hufford, M. B. (2019). The extent of adaptive wild introgression in crops. *New Phytologist*, *221*(3), 1279–1288. https://doi.org/10.1111/nph.15457

Jombart, T., & Ahmed, I. (2011). Adegenet 1.3-1: New tools for the analysis of genome-wide SNP data. *Bioinformatics*, *27*(21), 3070–3071. https://doi.org/10.1093/bioinformatics/btr521

Kane, N. C., King, M. G., Barker, M. S., Raduski, A., Karrenberg, S., Yatabe, Y., Knapp, S. J., & Rieseberg, L. H. (2009). Comparative genomic and population genetic analyses indicate highly porous genomes and high levels of gene flow between divergent *helianthus* species. *Evolution*, *63*(8), 2061–2075. https://doi.org/10.1111/j.1558-5646.2009.00703.x

Kess, T., Gross, J., Harper, F., & Boulding, E. G. (2016). Low-cost ddRAD method of SNP discovery and genotyping applied to the periwinkle

Littorina saxatilis. *Journal of Molluscan Studies*, *82*(1), 104–109. https://doi.org/10.1093/mollus/eyv042

Koboldt, D. C., Zhang, Q., Larson, D. E., Shen, D., McLellan, M. D., Lin, L., Miller, C. A., Mardis, E. R., Ding, L., & Wilson, R. K. (2012). VarScan 2: Somatic mutation and copy number alteration discovery in cancer by exome sequencing. *Genome Research*, *22*(3), 568–576. https://doi.org/10.1101/gr.129684.111

Kremer, A., & Hipp, A. L. (2020). Oaks: An evolutionary success story. *New Phytologist*, *226*(4), 987–1011. https://doi.org/10.1111/nph.16274

Larson, D. A., Vargas, O. M., Vicentini, A., & Dick, C. W. (2021). Admixture may be extensive among hyperdominant Amazon rainforest tree species. *New Phytologist*, *232*(6), 2520–2534. https://doi.org/10.1111/nph.17675

Lee-Yaw, J. A., Grassa, C. J., Joly, S., Andrew, R. L., & Rieseberg, L. H. (2019). An evaluation of alternative explanations for widespread cytonuclear discordance in annual sunflowers (*Helianthus*). *New Phytologist*, *221*(1), 515–526. https://doi.org/10.1111/nph.15386

Lefèbvre, C. (1969). Populations d'*Armeria* Willd. le long de la Mer Baltique et de la Mer du Nord. *Bulletin de la Société Royale de Botanique de Belgique*, *102*, 293–303. https://www.jstor.org/stable/20792690

Lefèbvre, C. (1974). Population variation and taxonomy in *Armeria maritima* with special reference to heavy-metal-tolerant populations. *New Phytologist*, *73*(1), 209–219. https://doi.org/10.1111/j.1469-8137.1974.tb04620.x

Leigh, J. W., & Bryant, D. (2015). Popart: Full-feature software for haplotype network construction. *Methods in Ecology and Evolution*, *6*(9), 1110–1116. https://doi.org/10.1111/2041-210X.12410

Leroy, T., Louvet, J. M., Lalanne, C., Le Provost, G., Labadie, K., Aury, J. M., Delzon, S., Plomion, C., & Kremer, A. (2020). Adaptive introgression as a driver of local adaptation to climate in European white oaks. *New Phytologist*, *226*(4), 1171–1182. https://doi.org/10.1111/nph.16095

Li, H., & Durbin, R. (2009). Fast and accurate short read alignment with burrows-wheeler transform. *Bioinformatics*, *25*(14), 1754–1760. https://doi.org/10.1093/bioinformatics/btp324

Li, H., Handsaker, B., Wysoker, A., Fennell, T., Ruan, J., Homer, N., Marth, G., Abecasis, G., & Durbin, R. (2009). The sequence alignment/map format and SAMtools. *Bioinformatics*, *25*(16), 2078–2079. https://doi.org/10.1093/bioinformatics/btp352

Liu, X., & Fu, Y.-X. (2015). Exploring population size changes using SNP frequency spectra. *Nature Genetics*, *47*(5), 555–559. https://doi.org/10.1038/ng.3254

Lotsy, J. P. (1925). Species or linneon. *Genetica*, *7*, 487–506. https://doi.org/10.1007/BF01676287

Marburger, S., Monnahan, P., Seear, P. J., Martin, S. H., Koch, J., Paajanen, P., Bohutínská, M., Higgins, J. D., Schmickl, R., & Yant, L. (2019). Interspecific introgression mediates adaptation to whole genome duplication. *Nature Communications*, *10*, 5218. https://doi.org/10.1038/s41467-019-13159-5

Martin, B. T., Chafin, T. K., Douglas, M. R., & Douglas, M. E. (2021). ClineHelpR: An R package for genomic cline outlier detection and visualization. *BMC Bioinformatics*, *22*(1), 501. https://doi.org/10.1186/s12859-021-04423-x

Mostert-O'Neill, M. M., Reynolds, S. M., Acosta, J. J., Lee, D. J., Borevitz, J. O., & Myburg, A. A. (2021). Genomic evidence of introgression and adaptation in a model subtropical tree species, *Eucalyptus grandis*. *Molecular Ecology*, *30*(3), 625–638. https://doi.org/10.1111/mec.15615

Nieto Feliner, G. (1990). Armeria. In S. S. Castroviejo, et al. (Eds.), *Flora Iberica* (Vol. *2*, pp. 642–721). Consejo Superior de Investigaciones Científicas.

Nieto Feliner, G. (1997). Natural and experimental hybridization in *Armeria* (Plumbaginaceae): *Armeria salmantica*. *International Journal of Plant Sciences*, *158*(5), 585–592. https://doi.org/10.1086/297471

Nieto Feliner, G., Álvarez, I., Fuertes, J., Heuertz, M., Marques, I., Moharrek, F., Piñeiro, R., Riina, R., Rosselló, J. A., Soltis, P. S., & Villa-Machío, I. (2017). Is homoploid hybrid speciation that rare? An empiricist's view. *Heredity*, *118*(6), 513–516. https://doi.org/10.1038/hdy.2017.7

Nieto Feliner, G., Casacuberta, J., & Wendel, J. F. (2020). Genomics of evolutionary novelty in hybrids and polyploids. *Frontiers in Genetics*, *11*, 792. https://doi.org/10.3389/fgene.2020.00792

Nieto Feliner, G., Fuertes, J., & Rosselló, J. A. (2001). A new species of *Armeria* (Plumbaginaceae) from southern Spain with molecular and morphometric evidence on its origin. *Botanical Journal of the Linnean Society*, *135*(1), 71–84. https://doi.org/10.1111/j.1095-8339.2001.tb02371.x

Nieto Feliner, G., Fuertes, J., & Rosselló, J. A. (2002). Reticulation or divergence: The origin of a rare serpentine endemic assessed with chloroplast, nuclear and RAPD markers. *Plant Systematics and Evolution*, *231*(1), 19–38. https://doi.org/10.1007/s006060200009

Nieto Feliner, G., Gutiérrez Larena, B., & Fuertes, J. (2004). Fine-scale geographical structure, intra-individual polymorphism and recombination in nuclear ribosomal internal transcribed spacers in *Armeria* (Plumbaginaceae). *Annals of Botany*, *93*(2), 189–200. https://doi.org/10.1093/aob/mch027

Nieto Feliner, G., Izuzquiza, A., & Lansac, A. R. (1996). Natural and experimental hybridization in *Armeria* (Plumbaginaceae): *A. Villosa* subsp. *carratracensis*. *Plant Systematics and Evolution*, *201*(1), 163–177. https://doi.org/10.1007/BF00989059

Nieto Feliner, G., Rosato, M., Alegre, G., San Segundo, P., Rosselló, J. A., Garnatje, T., & Garcia, S. (2019). Dissimilar molecular and morphological patterns in an introgressed peripheral population of a sand dune species (*Armeria pungens*, Plumbaginaceae). *Plant Biology*, *21*(6), 1072–1082. https://doi.org/10.1111/plb.13035

Ortego, J., Gugger, P. F., & Sork, V. L. (2018). Genomic data reveal cryptic lineage diversification and introgression in Californian golden cup oaks (section Protobalanus). *New Phytologist*, *218*(2), 804–818. https://doi.org/10.1111/nph.14951

Parchman, T. L., Gompert, Z., Braun, M. J., Brumfield, R. T., McDonald, D. B., Uy, J. A. C., Zhang, G., Jarvis, E. D., Schlinger, B. A., & Buerkle, C. A. (2013). The genomic consequences of adaptive divergence and reproductive isolation between species of manakins. *Molecular Ecology*, *22*(12), 3304–3317. https://doi.org/10.1111/mec.12201

Petit, R. J., Bodénès, C., Ducousso, A., Roussel, G., & Kremer, A. (2004). Hybridization as a mechanism of invasion in oaks. *New Phytologist*, *161*(1), 151–164. https://doi.org/10.1046/j.1469-8137.2003.00944.x

Petit, R. J., & Excoffier, L. (2009). Gene flow and species delimitation. *Trends in Ecology and Evolution*, *24*(7), 386–393. https://doi.org/10.1016/j.tree.2009.02.011

Pfeifer, B., Wittelsbürger, U., Onsins, S. E. R., & Lercher, M. J. (2014). PopGenome: An efficient Swiss army knife for population genomic analyses in R. *Molecular Biology and Evolution*, *31*(7), 1929–1936. https://doi.org/10.1093/molbev/msu136

Pfennig, K. S. (2021). Biased hybridization and its impact on adaptive introgression. *Trends in Ecology and Evolution*, *36*(6), 488–497. https://doi.org/10.1016/j.tree.2021.02.010

Pfennig, K. S., Kelly, A. L., & Pierce, A. A. (2016). Hybridization as a facilitator of species range expansion. *Proceedings of the Royal Society B: Biological Sciences*, *283*(1839), 20161329. https://doi.org/10.1098/rspb.2016.1329

Philipp, M., Madsen, H. E. S., & Siegismund, H. R. (1992). Gene flow and population structure in *Armeria maritima*. *Heredity*, *69*(1), 32–42. https://doi.org/10.1038/hdy.1992.91

Piñeiro, R., Aguilar, J. F., Munt, D. D., & Nieto Feliner, G. (2007). Ecology matters: Atlantic–Mediterranean disjunction in the sand-dune

shrub *Armeria pungens* (Plumbaginaceae). *Molecular Ecology*, *16*(10), 2155–2171. https://doi.org/10.1111/j.1365-294X.2007.03280.x

Piñeiro, R., Widmer, A., Fuertes, J., & Nieto Feliner, G. (2011). Introgression in peripheral populations and colonization shape the genetic structure of the coastal shrub *Armeria pungens*. *Heredity*, *106*(2), 228–240. https://doi.org/10.1038/hdy.2010.46

Pritchard, J. K., Stephens, M., & Donnelly, P. (2000). Inference of population structure using multilocus genotype data. *Genetics*, *155*(2), 945–959. https://doi.org/10.1093/genetics/155.2.945

Purcell, S., Neale, B., Todd-Brown, K., Thomas, L., Ferreira, M. A. R., Bender, D., Maller, J., Sklar, P., de Bakker, P. I. W., Daly, M. J., & Sham, P. C. (2007). PLINK: A tool set for whole-genome association and population-based linkage analyses. *The American Journal of Human Genetics*, *81*(3), 559–575. https://doi.org/10.1086/519795

R Core Team. (2015). *R: A language and environment for statistical computing*. R Foundation for Statistical Computing. Retrieved from. https://www.r-project.org/

Rieseberg, L. H. (1995). The role of hybridization in evolution: Old wine in new skins. *American Journal of Botany*, *82*(7), 944–953. https://doi.org/10.1002/j.1537-2197.1995.tb15711.x

Rieseberg, L. H., & Wendel, J. F. (1993). Introgression and its consequences in plants. In R. Harrison (Ed.), *Hybrid zones and the evolutionary process* (pp. 70–109). Oxford University Press.

Sætre, G. P. (2013). Hybridization is important in evolution, but is speciation? *Journal of Evolutionary Biology*, *26*, 256–258. https://doi.org/10.1111/jeb.12005

Schmitt, S., Hérault, B., Ducouret, E., Baranger, A., Tysklind, N., Heuertz, M., Marcon, E., Cazal, S. O., & Derroire, G. (2020). Topography consistently drives intra- and inter-specific leaf trait variation within tree species complexes in a neotropical forest. *Oikos*, *129*, 1521–1530. https://doi.org/10.1111/oik.07488

Schmitt, S., Tysklind, N., Hérault, B., & Heuertz, M. (2021). Topography drives microgeographic adaptations of closely-related species in two tropical tree species complexes. *Molecular Ecology*, *30*(20), 5080–5093. https://doi.org/10.1111/mec.16116

Scott, P. A., Glenn, T. C., & Rissler, L. J. (2019). Formation of a recent hybrid zone offers insight into the geographic puzzle and maintenance of species boundaries in musk turtles. *Molecular Ecology*, *28*(4), 761–771. https://doi.org/10.1111/mec.14983

Stebbins, G. L. (1971). *Chromosomal evolution in higher plants*. Edward Arnold.

Suarez-Gonzalez, A., Hefer, C. A., Lexer, C., Cronk, Q. C., & Douglas, C. J. (2018). Scale and direction of adaptive introgression between black cottonwood (*Populus trichocarpa*) and balsam poplar (*P. balsamifera*). *Molecular Ecology*, *27*(7), 1667–1680. https://doi.org/10.1111/mec.14561

Suarez-Gonzalez, A., Lexer, C., & Cronk, Q. C. (2018). Adaptive introgression: A plant perspective. *Biology Letters*, *14*(3), 20170688. https://doi.org/10.1098/rsbl.2017.0688

Tauleigne-Gomes, C., & Lefèbvre, C. (2005). Natural hybridisation between two coastal endemic species of *Armeria* (Plumbaginaceae) from Portugal. 1. Populational in situ investigations. *Plant Systematics and Evolution*, *250*(3–4), 215–230. https://doi.org/10.1007/s00606-004-0247-7

Tauleigne-Gomes, C., & Lefèbvre, C. (2008). Natural hybridisation between two coastal endemic species of *Armeria* (Plumbaginaceae) from Portugal. 2. Ecological investigations on a hybrid zone. *Plant Systematics and Evolution*, *273*(3–4), 225–236. https://doi.org/10.1007/s00606-008-0019-x

Tsitrone, A., Kirkpatrick, M., & Levin, D. A. (2003). A model for chloroplast capture. *Evolution*, *57*, 1776–1782. https://doi.org/10.1111/j.0014-3820.2003.tb00585.x

Turesson, G. (1922). The genotypical response of the plant species to the habitat. *Hereditas*, *3*, 211–350.

Vitelli, M., Vessella, F., Cardoni, S., Pollegioni, P., Denk, T., Grimm, G. W., & Simeone, M. C. (2017). Phylogeographic structuring of plastome diversity in Mediterranean oaks (*Quercus* group *ilex*, Fagaceae). *Tree Genetics and Genomes*, *13*(1), 1–17. https://doi.org/10.1007/s11295-016-1086-8

Wang, X., Chen, L., & Ma, J. (2019). Genomic introgression through interspecific hybridization counteracts genetic bottleneck during soybean domestication. *Genome Biology*, *20*(1), 1–15. https://doi.org/10.1186/s13059-019-1631-5

Wendel, J. F., Schnabel, A., & Seelanan, T. (1995). An unusual ribosomal DNA sequence from *Gossypium gossypioides* reveals ancient, cryptic, intergenomic introgression. *Molecular Phylogenetics and Evolution*, *4*(3), 298–313. https://doi.org/10.1006/mpev.1995.1027

Zhang, W. P., Cao, L., Lin, X. R., Ding, Y. M., Liang, Y., Zhang, D. Y., Pang, E. L., Renner, S. S., & Bai, W. N. (2022). Dead-end hybridization in walnut trees revealed by large-scale genomic sequence data. *Molecular Biology and Evolution*, *39*(1), msab308. https://doi.org/10.1093/molbev/msab308

SUPPORTING INFORMATION

Additional supporting information can be found online in the Supporting Information section at the end of this article.

How to cite this article: Villa-Machío, I., Heuertz, M., Álvarez, I., & Nieto Feliner, G. (2023). Demography-driven and adaptive introgression in a hybrid zone of the *Armeria* syngameon. *Molecular Ecology*, *00*, 1–16. https://doi.org/10.1111/mec.17167